

Optical Properties of Y_2O_3 -Doped ZnO Thin Films Sputtered in an Ar:O₂ Gas RF Magnetron Sputtering Technique.

Sowjanya M.^{1*}, Pamu D.¹, Chowdhruy R.³ and Jayaganthan R.⁴

¹Centre of Nanotechnology, Indian Institute of Technology Roorkee, Roorkee 247 667, India

²Department of Physics, Indian Institute of Technology Guwahati, Guwahati 781 039, India

³Department of Civil Engineering, Indian Institute of Technology Roorkee, Roorkee 247 667, India

⁴Department of Metallurgical and Materials Engineering, Indian Institute of Technology Roorkee, Roorkee 247 667, India
E-mail: sowjiphysics@gmail.com

Abstract—In this work, the Y_2O_3 doped zinc oxide (ZnO) thin films were deposited on SiO_2 substrate by using the radio frequency magnetron sputtering technique (RF sputtering). The microstructures and optical properties of the thin films deposited using different gas (Ar:O₂) ratio at 400 °C were characterized. XRD analysis of thin films has shown that all the fabricated films are polycrystalline and single phase hexagonal wurtzite—type structure with a strong (002) orientation. Y_2O_3 doped ZnO thin films exhibits denser morphology with refined microstructure as compared to pure films. The increase of O₂ gas mixture causes the decrease of the intensity of peak (002). The transmittance and absorbance of doped ZnO thin films were measured by UV-VIS-IR spectrophotometer in the wavelength range 300 nm to 800 nm. The high transmittance in visible region and large band gap of the films were observed. Photoluminescence (PL) of the films was measured at the excitation wavelength of 325 nm and it has revealed the two PL peaks in UV and visible regions (400 nm to 445 nm). The Ar:O₂ gas ratio affects the stoichiometry, structural, and optical properties of the Y_2O_3 doped ZnO thin films as observed in the present work.

Keywords: RF Sputtering, ZnO, Y_2O_3 , XRD, AFM, Photoluminescence

1. INTRODUCTION

Transparent oxide ZnO is semiconducting material that has a direct band gap of 3-3.37 eV and with a large excitation binding energy (60 meV) at room temperature [1]. ZnO is widely used material because of it is less expensive and abundantly available compound on earth. It is chemically and thermally stable in nature [2]. ZnO is a promising material in optoelectronic devices due to their potential applications in gas sensors, light emitting devices, piezoelectric transducers and in solar cells [3]. Materials such as ZnO and GaN are direct wide band gap ($E_g > 3$ eV) semiconductors, transparent in the visible region, having, wurtzite crystal structures, comparable lattice constant, with nearly same c/a (ideal axial ratio) lattice constant ratios [5]. Both of the these

semiconductor are owe defect related deep level visible (PL) emissions [4,5].

Y_2O_3 -doped ZnO are attracted many researchers to study their microstructure and electrical characteristics. Y_2O_3 -doped ZnO ceramics used for the formation of a grained Y_2O_3 containing phase along the grain boundaries of the ZnO grain which inhibits the grain growth. The threshold voltage of the ceramics increasing from 150 to 274 Vmm, the leakage current also increased with the amount of Y_2O_3 added, and nonlinear coefficient (α) was not influenced and remained at approximately 40 [6]. Park et al., [7] investigated that the effect of Y_2O_3 and contents on the microstructure and electrical properties of Pr_6O_{11} based ZnO varistor. The nonlinear coefficient (α) and the average grain size increased with increasing the Y_2O_3 contents, whereas the dielectric constant (ϵ) decreased, the highest nonlinearity, with nonlinear coefficient (α) of 77, and with the dielectric constant 352 at 1kHz.

In another work, Nahm et al., [8] studied on the microstructure and electrical properties of various Y_2O_3 -doped ZnO- Pr_6O_{11} based ceramics in detail as stated by them. Y_2O_3 enhances the inhibition of grain growth. An extensive literature as discussed above indicate that among the rare earth oxides doped ZnO varistor ceramics, Y_2O_3 can largely inhibit the growth of ZnO grains, So that the threshold voltage of ZnO-based varistor ceramics are remarkably improved properties. But there is no much available literature on the varistor properties of Y_2O_3 -doped based thin films. The significance for the further study of rare earth oxides doped ZnO thin films have lot of scope. Thus, it is essential to work on Y_2O_3 -doped ZnO thin films.

In this work, the Y_2O_3 -doped ZnO films were prepared by RF sputtering process on SiO_2 substrate. Further, the optical properties of thin films are studied in widespread ways which are very important for many applications such as in solar cells,

optical detectors, and optoelectronic devices due to their high stability [13]. Y₂O₃-doped ZnO thin films also have major role in microelectronics, optical sensor technology. These structures consist of high absorption coefficient [14]. Researchers have found that the optical properties strongly depend on the thickness of ZnO films. The optical properties of ZnO thin films vary between the various studies. The band gap values reported in the literature are extending from 2.0 eV up to 3.7 eV. ZnO films have been prepared by different deposition methods, such as sputtering [15], laser ablation [16], evaporation [17], spray and flame techniques [18], chemical vapour deposition [19] and sol gel [20,21]. Among all these methods, sputtering is one of the most versatile deposition techniques used for the deposition of transparent conduction oxides (TCO). Sputtering process produces layers with higher purity and better-controlled composition when compare with other processes. It also produces films with greater adhesive strength, homogeneity and it also permits better control of film thickness. Moreover, this technique is easy to deposit materials which could not be easily deposited using other techniques. In this paper, we introduce an investigation of the influence of the various Ar:O₂ sputtering gas ratio on the properties of Y₂O₃ doped ZnO thin films. It is well known that the Ar:O₂ sputtering ratio has considerable influence on the optical properties of deposited films. The optical energy gap (*E_g*). Photoluminescence (PL) of the films was measured at the excitation wavelength of 325 nm.

2. EXPERIMENTAL DETAILS

2.1. Preparation of Y₂O₃-doped target and ZnO thin films

In this study, we have successfully deposited Y₂O₃-doped ZnO, thin films on SiO₂ substrate in the Argon (Ar) gas (99.99% purity) and oxygen gas (99.99% purity) atmosphere, using RF sputtering technique. The target of Y₂O₃-doped ZnO was prepared by the solid state reaction method. Via mixing of Y₂O₃ (99.99% purity) and ZnO (99.98% purity) powders in stoichiometric ratios which was 1:50 for 2% Y₂O₃-doping. The powders were toughly mixed and grained for 6 h. Polymer solution of polyvinyl alcohol (PVA) with concentration of ~3% was used as the binder. These homogenous powders were pressed in to a disk, called pallets of diameter of 20 mm and the thickness about 5 mm by applying pressure. The powders were then uniaxial pressed target of 62 mm diameter and sintered at 1000 °C for 3 h in the air to form the RF sputtering target of Y₂O₃-doped ZnO. The SiO₂ substrates were initially cleaned in an ultrasonic bath and then washed with acetone and stored for further use. Deposition parameters were optimized by obtaining the highly oriented thin films. The deposition of the films was carried out at room temperature, 400 °C on SiO₂ substrates at different sputtering gas Ar:O₂, quantified in terms of standard cubic centimeters per minute (SCCM), and a fixed power of 80 W for 3 h under the sputtering gas pressure of 2.5×10⁵ mbar. The sputtering process was carried out in various Ar and O₂ atmosphere with deposition time of 3 hours. The deposition time was

maintained constant for all the samples. The operating parameters used during sputtering deposition are shown in Table 1. The distance maintained among target and substrate was ~4.5 cm, the various sputtering gas (Ar to O₂) ratios used were (20:0, 15:5, 10:10, 5:15 and 0:20). The optimized parameters, i.e. the temperature and pressure of deposition for these thin films are given in Table 1. To improve the crystallinity of thin films, we have done post deposition.

Table 1: Sputtering deposition parameters and materials used

Description	Value or Parameter
Target prepared	Y ₂ O ₃ -doped-ZnO
Substrate used	SiO ₂
Base pressure	2.5×10 ⁵ mbar
Working pressure	3.0×10 ⁻² mbar
Power supplied	80 w
Distance between target and substrate	4.5 cm
Temperature	400 °C
Deposition time	3h

Table 2: Variation of grain size, FWHM, d-spacing, lattice parameter and for doped and undoped ZnO thin films on SiO₂ substrates.

Name (Thin films)	h k l	2θ°	FWHM	d-spacing (Å)	D (nm)	Lattice parameter (c)
Y ₂ O ₃ -doped ZnO(pallet)	0 0 2	34.5137	0.1080	2.59661	27.73	5.19322
Y ₂ O ₃ -doped ZnO(thinfilms)	0 0 2	34.4371	0.1596	2.60221	18.02	5.20442

2.2. Characterization of the thin films

Structural characterizations of these thin films were examined by X-ray diffract meter model (Model: D8 ADVANCE, Bruker) in 2θ mode, with CuKα radiation (λ=0.154 nm). The source of X-ray operated at a power of 40 kV 30 mA. The surface topography and roughness of the as grown films were examined by atomic force microscopy (AFM; NT-MDT: Model NTEGRA) in semi-conduct mode with the silicon nitride tip of radius 10 nm. The grain morphology and the chemical composition from energy dispersive analysis of X-rays (EDX) of the thin film samples was examined by field emission scanning electron microscopy (FESEM; Model: Quanta 200F FEG and FEI Netherlands) with a very high electric potential of 20 kV. The optical properties transmittance, absorbance and reflectance for these thin films were observed by (Varian Cary 500 UV-VIS NIR) spectrophotometer. The optical band gap was calculated from the Talc's plot (αhv)² versus hv. Photoluminescence (PL) spectra were obtained for the films by using spectrofluorophotometer (SHIMAZDU, Model: RF-5301PC) with 150W xenon lamp, ozone resolving type lamp housing and operating temperature at 25 °C. The light source of Xe lamp at the excitation wavelength of 325 nm was used for PL

study. All the measurements were performed in air at room temperature.

3. RESULTS AND DISCUSSIONS

3.1. Structural properties

3.1.1. XRD analysis

Fig. 1(a and b) represents the XRD patterns of Y_2O_3 doped ZnO pellets and thin films respectively. Fig. 1(a) represents the XRD plot of Y_2O_3 doped ZnO pellets and were sintered at 1000 °C. The XRD peaks of thin film deposited on the SiO_2

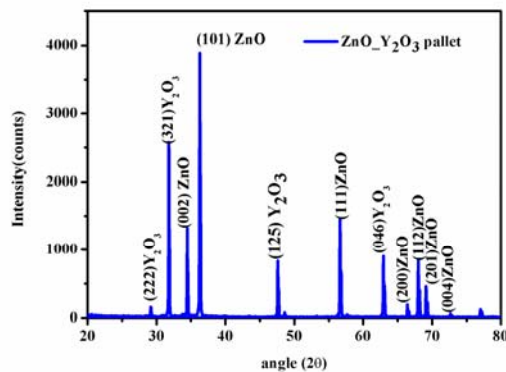


Fig. 1(a). XRD plot of Y_2O_3 doped ZnO pallet sintering at 1000°C

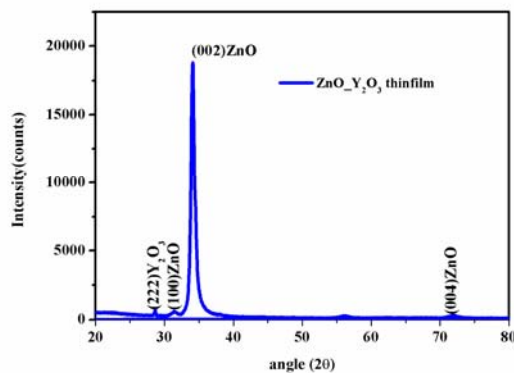


Fig. 1(b): XRD plot of Y_2O_3 doped ZnO thin films on SiO_2 substrate at 400 °C.

substrate in $Ar:O_2$ atmospheres at 400 °C which are shown in the Fig. 1(b). As observed from the Fig 1(b) the XRD patterns were polycrystalline films with hexagonal (wurtzite) structure. It can be also seen that from Fig. 1(b) the intensity for the entire plane remained highest for Y_2O_3 -doped ZnO. The diffractogram that the peak at (002) planes dominates the other peaks appearing clearly indicating the superior orientation of thin films or pellet along the c -axis. The growth patterns of the Y_2O_3 doped ZnO thin films were at right angles to SiO_2 substrate. The polycrystalline films with hexagonal (wurtzite) structure were observed for pellet and doped thin films in the range of 20–80°. The major peak (002) was observed at 34.4°

for both Y_2O_3 doped ZnO thin films and pellet. The average crystalline sizes of the thin films deposited on SiO_2 substrate have been calculated using the Scherer's equation as shown below:

$$D = \frac{0.9\lambda}{\beta \cos \theta} \quad (1)$$

where λ is the wavelength of X-rays used at $\lambda = 0.154$ nm, for Cu $K\alpha$ target and θ is the Bragg's diffraction angle of the peak (002). For the hexagonal lattice, lattice spacing d is given by the below specified relation:

$$\frac{1}{d^2} = \frac{4}{3} \left(\frac{h^2 + hk + k^2}{a^2} \right) + \frac{l^2}{c^2} \quad (2)$$

where h , k , and l are Miller indices of the plane and a and c are the lattice constant for the hexagonal unit cell. From Eq (2) values for the lattice constants a and c are calculated.

3.1.2. FE-SEM and EDX analysis

The field emission scanning microscopic (FE-SEM) study was carried for the surface morphology of the thin film with Y_2O_3 -doped (2 at.%) ZnO and Fig 2 (a) represents the same. From the Fig. 2 (a), very fine grain averaging to near 32 nm are observed and distributed evenly with high uniformity throughout. The uniform distribution is the result of controlled preferential nucleation of the grains drive by RF sputtering deposition process. Films have uniform density and composed of randomly oriented grains. The grains are very smaller and more elongated in thin film prepared with lower Y_2O_3 concentration. The grain size increases and the shape of the grains become round and hexagonal with increasing precursor concentration as observed in Fig. 2(a).

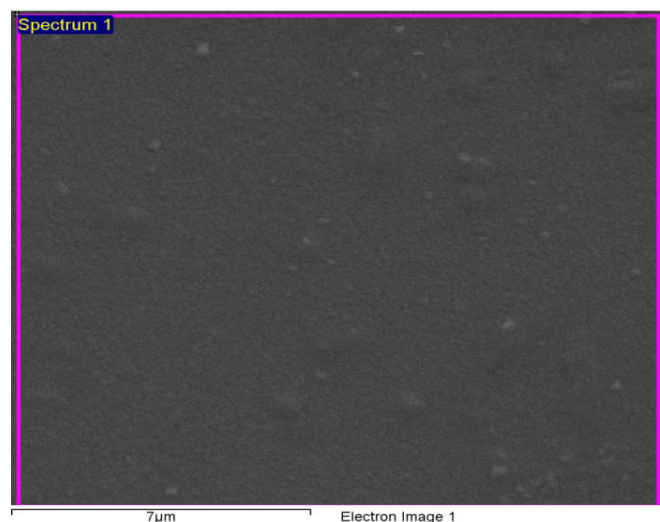


Fig. 2(a): FE-SEM image of Y_2O_3 doped ZnO thin films deposited on SiO_2 substrate at 400 °C.

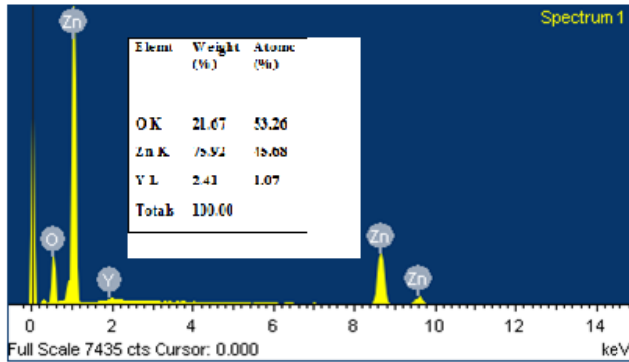


Fig.2 (b): EDX of Y_2O_3 doped ZnO thin films deposited on SiO_2 substrate at 400 °C.

Similarly, Fig. 2(b) indicates the EDX spectra of Y_2O_3 doped ZnO thin films prepared by RF sputtering. The main idea of the EDX analysis in this study is to identify the elements presents in the deposited thin film after the calcination. As observed from Fig. 2(b), the elements such as Zn, Y and O are present in thin film. Even after calcination of target at ~ 1000 °C and deposited the thin films at 400 °C by sputtering, elements were remained unchanged which confirms the originally prepared materials in its original state.

3.1.3. AFM analysis

Atomic force microscopy (AFM) was used to study the surface topography of Y_2O_3 doped ZnO thin films. Fig. 3(a) shows the 2 dimensional AFM image of the sample deposited on SiO_2 substrate. The anisotropic grain growth may occur in thin films due to the factors such as preferred orientation of the grains, orientation-dependent grain boundary mobility and grain boundary free energy, and residual stress which gives an excellent measure of the smooth film fabricated with a high homogeneity. As shown in 3D image of the Fig. 3 (b), uniform and homogenous crystallite distribution results in the enchased film transparency. Fig 3 (c) is the histogram of the AFM image. The average roughness is 13.147 nm and RMS 17.385 nm roughness and grain size of the thin film results reported.

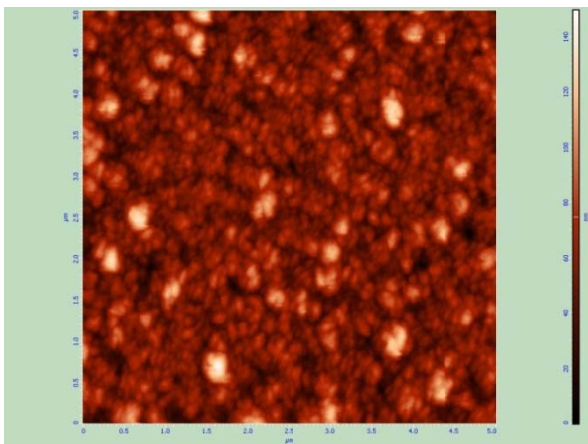


Fig. 3(a): AFM 2D image of Y_2O_3 doped ZnO thin film deposited on SiO_2 substrate at 400 °C.

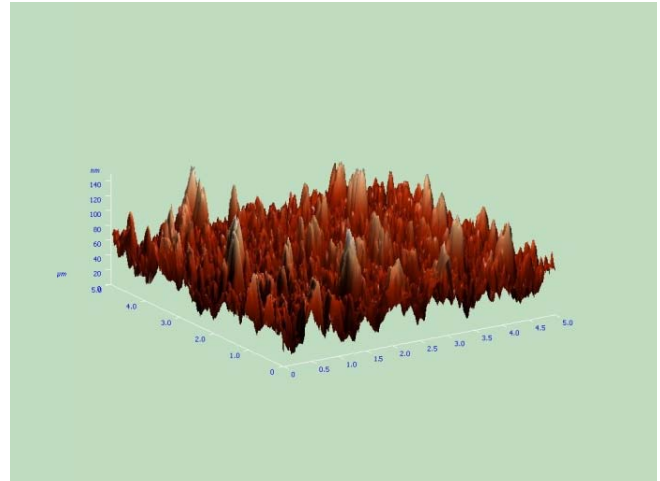


Fig. 3(b): AFM 3D image of Y_2O_3 doped ZnO thin film deposited on SiO_2 substrate at 400 °C.

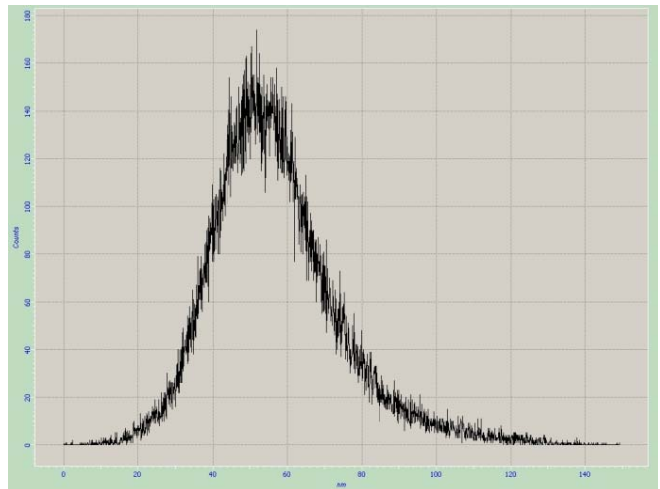


Fig. 3(c): AFM image of Y_2O_3 doped ZnO thin film histogram deposited on SiO_2 substrate at 400 °C.

3.2. Optical measurement

The optical absorbance is shown in Fig. 4 (a) in the wave length range between 300-800 nm at various Ar: O_2 ratios. The optical absorbance of different Ar: O_2 ratios (20:0), (15:5), (10:10), (5:15), (0:20) between 0 to 50% in near-UV spectral region ranges from 400 nm down to 300 nm. The absorbance less than 50% below the energy band gap, the absorption is caused by the defects states. The absorption edge shifts towards longer wave lengths in the increasing Ar: O_2 ratios the thin film thickness decreasing indicating a decreasing in the band gap. It is also revealed that with increase in argon to oxygen ratio, the absorbance value decreases.

The reflectance spectrum is demonstrated in Fig. 4 (b) in the spectra range of 300 to 800 nm. From the figure it is clear that the reflectance quite low in all the samples. The change in optical reflectance may be due to the morphological change in films, as the aspect ratio of crystallites changes with sputtering

Ar:O₂ gas ratios decreasing then thin film thickness also in decreasing. The optical transmittance spectra as shown in Fig. 4.(c) in the wave length 300 to 800 nm, the average transmittance achieved in the visible range was very high for various Ar:O₂ gas ratios. These curves show a well defined interference fringe pattern, indicating the smooth surface of the thin films. These thin films suitable for application as the window layer for solar cell fabrication and transparent electromagnetic interference (EMI) shielding materials. From the transmittance data absorption coefficient α can be calculated using Lamber's formula [22].

$$\alpha = \frac{1}{t \left[\ln(t/T_r) \right]} \tag{3}$$

where T_r and t are the optical transmittance and thickness of the thin film, respectively. The optical band gap of thin films was calculated. Based on the theory of optical transmission, the relationship between the absorption coefficient (α) and photon energy of the incident light ($h\nu$) for direct transition is given by the below equation:

$$(\alpha h\nu)^n = A(h\nu - E_g) \tag{4}$$

where A is constant, E_g is band gap in eV. For $n=1/2$ the transition data provide the best linear fit in the band-edge region, implying the transition is direct in nature. The direct band gaps of the films were calculated from the $(\alpha h\nu)^2$ vs. $h\nu$ (Tauc model) plot by extrapolating a fit of the linear region to $\alpha=0$, as shown in Fig. 4(d). The linear dependence of $(\alpha h\nu)^2$ with $h\nu$ indicates that Y₂O₃ doped ZnO thin films are direct transition type semiconductors. The optical band gap of thin films lies in the range between 3.366 eV and 3.038 eV. The observed band gap values are almost increased with increasing the argon gas concentration. The values of Y₂O₃ doped ZnO thin films deposited at different Ar:O₂ ratios are as follows: for 0:20 (3.061 eV), 5:15 (3.038 eV), 10:10 (3.055 eV), 15:5 (3.169 eV), and 20:0 (3.366 eV).

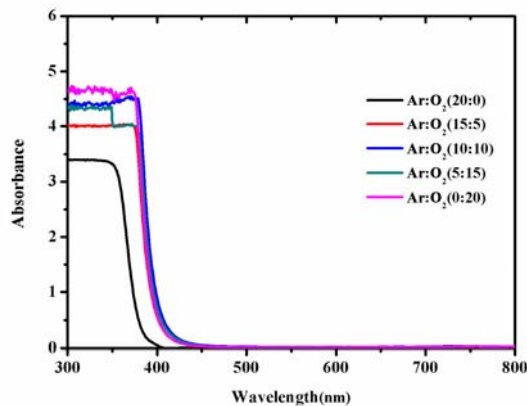


Fig. 4(a): Wavelength versus absorbance Y₂O₃ doped ZnO thin films deposited on SiO₂ substrate at 400 °C.

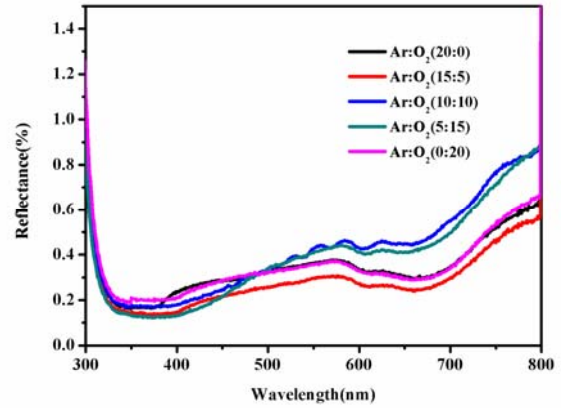


Fig. 4(b): Wavelength versus Reflectance for Y₂O₃ doped ZnO thin films deposited on SiO₂ substrate at 400 °C.

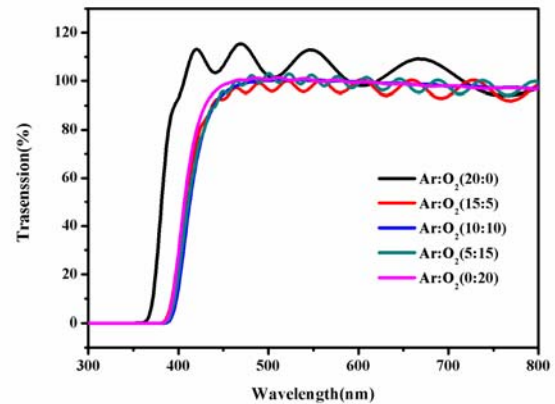


Fig. 4(c): Wavelength versus transmittance plots for Y₂O₃ doped ZnO thin films deposited on substrate at 400 °C

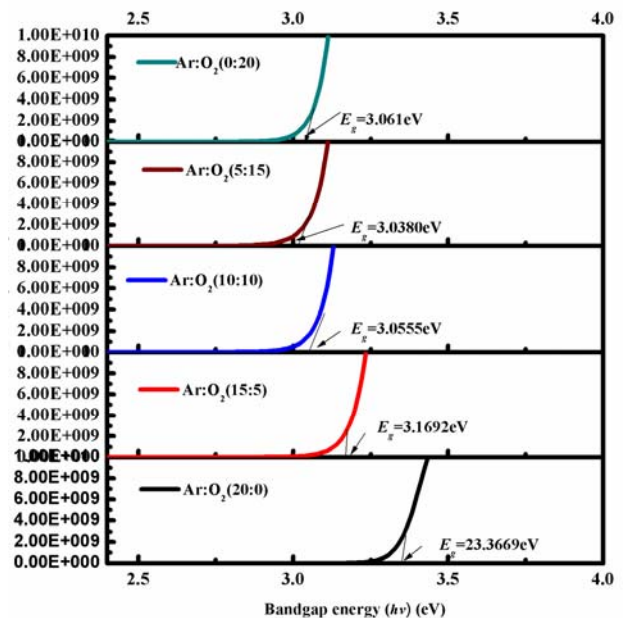


Fig. 4(d): Plot of $(\alpha h\nu)^2$ versus $(h\nu)$ for Y₂O₃ doped ZnO thin films deposited on SiO₂ substrate at 400 °C.

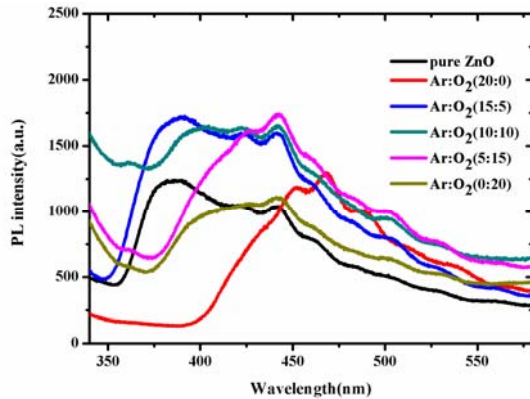


Fig. 4(e): PL bands of undoped ZnO thin film on SiO_2 substrate and La_2O_3 doped ZnO thin films at different Ar to O_2 ratios on SiO_2 substrate and at $400^\circ C$.

3.3. Photoluminescence (PL)

Photoluminescence (PL) is the emission of the light after the absorption of the electromagnetic radiation. It is generally known that the intensities of the PL spectrum provide the information about the optical band gap, defects and the quality of the deposited films. PL spectra were obtained for all deposited thin films. PL emission studies at room temperature for Y_2O_3 doped ZnO thin films with different (Ar: O_2) sputtering gas ratios (20:0), (15:5), (10:10), (5:15), (0:20) carried out in the wavelength range of 300 to 600 nm and at the excited wavelength of 330 nm. All the spectra exhibited a broad peak at nearly 389 nm with less intense secondary emission at 400 to 445 nm. The PL intensity was observed to be more for sputtering gas (Ar: O_2) ratio for 15:5 out of (20:0), (10:10), (5:15), and (0:20). The defects that are created due to different Ar: O_2 gas proportions strongly influence the PL emission. The peak at 350 to 450 nm in all the cases may be due to the prances of the Zn vacancies. The results are in good agreement with the previous PL results on thin films [24,25].

4. CONCLUSIONS

In this study Y_2O_3 doped ZnO thin films of varying (Ar: O_2) RF sputtering gas ratios were successfully deposited on SiO_2 substrate. The deposited thin films are single phased with prudential growth in (002) plane, along the c-axis. Polycrystalline films with hexagonal (wurtzite) structure are observed. The surface topography studies from AFM and FESEM images describe that the grains are uniformly grown on the film surface. The surface of thin films is reasonably smooth with small values of average and RMS roughness. The deposited thin films show good optical characteristics, very high optical transmittance in the visible region, low optical reflection exhibit a sharp absorption edge at a wavelength below 400 nm, hence Y_2O_3 doped ZnO lowers the band gap. The large values of optical transmittance enable application of Y_2O_3 doped ZnO thin films for transparent window layer of solar cells. Photoluminescence (PL) spectra show sharp peaks in the UV and visible regions. Due to visible emission peaks

Y_2O_3 doped ZnO thin films find optical applications such as LEDs, window layer for solar cell fabrication and transparent electromagnetic interference (EMI) shielding materials, and laser diodes. The Y_2O_3 -doped ZnO thin films exhibit excellent optical properties, and are applicable for fabrication of optoelectronic devices.

5. ACKNOWLEDGMENTS

The authors thank CSIR for financial support as JRF/SRF fellowship. We also thank Computer Center, Mahatma Gandhi Central Library and Institute Instrumentation Centre of IIT Roorkee for providing necessary facilities. SM extends her acknowledgments to IIT Guwahati for providing experimental facilities. Sincere thanks to Mr. Mahesh, Ms. Pallabi, Mr. Anil Kumar, Dr. P. Rajendra and Dr. T. Santosh Kumar for their help and support during experimentation

REFERENCES

- [1] B.K. Sharma, N. Khare, D. Haranath, Solid State Commun. 150 (2010) 2341–2345.
- [2] X. Y. Li, H.J. Li, Z.J. Wang, H. Xing, J.X. Wang, B.C. Yang, Opt.Commun.282(2009) 247–252
- [3] R.K. Shukla, A. Srivastava, A. Srivasa, K.C. Dubey, J. Cryat. Growth 294 (2006) 42–431.
- [4] K. Adhikary, S. Chudhuri, Trans. Ind.Ceram. Soc.66(2007)1–16.
- [5] M.A. Reshchikov, H. Morkoc, J. Appl. Phy.97 (2005)061301_061395.
- [6] BERNIK S, MACEK S, AI B. Micro structural and electrical characteristics of Y_2O_3 -doped ZnO/ Bi_2O_3 based varistor ceramics [J].Journal of the European Ceramics Society,2001.21(10_11): 1875_1878.
- [7] PARKJ S, HAN Y H, CHOI K H. Effects of Y_2O_3 on the microstructure and electrical properties Journal of Materials Science : Materials in Electronics, 2005, 16(4): 215–219.
- [8] NAHM C W. Effect of cooling rate on degradation characteristics of ZnO-Pr6O11-CoO-Cr2o3-Y2O3-based varistors [J]. Solid state Communications, 2004,132(3-4); 213-218.
- [9] NAHM C W. Microstructure and electrical properties of Y_2O_3 -doped ZnO-PR6O11 BASED VARISTOR CERAMICS [J]. Materials Letters, 2003,57(7):1317-1321.
- [10] NAHM C W, PARK C H. Microstructure, electrical and degradation behavior of praseodymium oxides-based zinc oxide varistors doped with y_2o_3 [J]. Journal of Materials Science, 2000, 35(12):3037-3042.
- [11] NAHM C W, SHINB C. Effect of sintering time on electrical properties and stability against DC accelerated aging of Y_2O_3 -doped ZnO-Pr6O11 -based varistor ceramics [J].Ceramics International, 2004,30(1): 9-15.
- [12] NAHM C W, SHIN B C. Highly stable nonlinear properties of [J], ceramics ZnO-Pr6O11-CoO-Cr2O3-Y2O3-based varistor Materials Letters, 2003,57(7): 1322-1326.
- [13] Chowdhury R, Adhikari S, Rees P (2010). Optical properties of silicon doped ZnO. Physica. B, 405: 4763-4767.

-
- [14] Kim YI, Seshadri R (2008).Optical properties of Cation-substituted Zinc Oxide. *Inorg. Chem.*, 8437-8443.
- [15] X. Jiang, F. L. Wong, M. K. Fung, S. T. Lee, *Appl. Phys.Lett.*83(2003)498.
- [16] Y.F. Lu, H. Q. Ni, Z.M. Ren, *J. Appl. Phys.* 88 (2000) 498.
- [17] P.Petrou, R. S INGH, D. E. Brodie, *Appl. Phys. Lett.* 35 (1979)930.
- [18] P. Nunes, E. Fortunadeo, R. Martins, *Thin Solid Films* 383 (2001) 277
- [19] E. Jimenez-Gonzalez, A. Jose, R. Suarez-Parra, *J. Cryst. Growth* 192 (1998) 430.
- [20] Lidia Armelao, F. Monica Fabrizio, G. Stefano Gialanella, Z. Fiorenzo Zordan, *Thin Solid Films* 394 (2001) 90.
- [21] Z. Ben Ayadi, L. ElMir, K. Diessas, s. Alaya, *Nanotechnology* Fiorenzo Zordan, *ThinFilms* 394 (2001) 90.
- [22] Y.J. Choi,S.C. Gonga, D.C. Johnson, S.Golledge, G.Y. Yeom, H. H. Park, *Appl. Surf. Sci.* 269 (2013) 92-97.
- [23] X. L i, H.Zhu,J. Wei, K. Wang, E. Xu, Z. Li, D. Wu, *Appl. Phys. A* 97 (2009) 341-344.
- [24] A. R. Babar, P. R. Deshamukh, R. J. Deokate, D. Haranath, C. H. Bhosale, K. Y. Rajpure, *J. Phys. D: Appl. Phys.* 41 (2008) 135404.
- [25] Noriko Saito, Haneda , Takashi Sekiguchi, Takamasa Ishigaki, Kunihito Koumoto, *Jour. of Electrochem. Soc.*, 151(2004) H169-H173.